

## Preparation of laser induced periodic surface structures for gas sensing thin films and gas sensing verification of a NiO based sensor structure

Ivan Hotovy<sup>2</sup>, Johann Zehetner<sup>1</sup>, Vlastimil Rehacek<sup>2</sup>, Miroslav Mikolasek<sup>2</sup>,  
Ivan Kostic<sup>4</sup>, Stanislava Serecunova<sup>2,3</sup>, Dana Seyringer<sup>1</sup>, Fadi Dohnal<sup>1</sup>

This study presents different approaches to increase the sensing area of NiO based semiconducting metal oxide gas sensors. Micro- and nanopatterned laser induced periodic surface structures (LIPSS) are generated on silicon and Si/SiO<sub>2</sub> substrates. The surface morphologies of the fabricated samples are examined by FE SEM. We select the silicon samples with an intermediate Si<sub>3</sub>N<sub>4</sub> layer due to its superior isolation quality over the thermal oxide for evaluating the hydrogen and acetone sensitivity of a NiO based test sensor.

Keywords: laser ablation, laser induced periodic surface structure, NiO, gas sensing

### 1 Introduction

Recently, we have noted great efforts by researchers to prepare new gas sensors as well as to integrate them into electronically controlled sensor arrays [1] seeking to improve their sensitivity and selectivity in different applications such as food quality control [2] environmental monitoring [3], non-invasive disease diagnosis [4] or detection of explosive and toxic gases for humans in dangerous concentrations [5]. Everywhere we see the need to identify small amounts of chemicals in the gaseous state. Over the last forty years of development, gas sensors based on various technologies, including thin films based on metal oxides, nanowires and nanotubes, have proven to have a considerable potential for detecting a wide range of chemical compounds. Gas sensors connected in sensor arrays and prepared on flexible substrates are characterized by excellent electrical conductivity, mechanical stability and low weight, while also becoming an essential part of portable devices and intelligent robots [6]. Attention of scientists is focused on altering the surface morphology of high aspect ratio structures so that the real surface area is greater than the geometrical area [7-9]. Then the increase of surface morphology often enhances the element functionality and reliability. A large real surface area can be achieved either by preparing small particles or clusters of particles (clusters) or by creating materials with pores in the surface [7].

In the present study, laser ablation was selected for contour shaping, surface patterning and surface functionalization due to its all-purpose applicability for a great variety of standard materials and new advanced materials essential for specific applications. We investigate the merits and drawback of different fabrication strategies in generating LIPSS [10] to increase the surface area for gas sensor application. It was important to obtain an electrically well insulated support surface for the NiO and Pt-based integrated electrodes. In our experiments we observed that the laser ablation process creates issues for thermal generated SiO<sub>2</sub> isolation layer. Alternatively, Si<sub>3</sub>N<sub>4</sub> was used for the isolation layer of the test sensor to verify the H<sub>2</sub> and acetone sensing characteristic.

### 2 Experimental details and results

In the first approach we intended to generate LIPSS directly on a Si/SiO<sub>2</sub> wafer. The wafer was thermally oxidised prior to the laser process and the oxide layer had a thickness of 350 nm. However, we could not successfully generate LIPSS directly on a Si/SiO<sub>2</sub> substrate. Due to the significant lower ablation threshold of Si with respect to SiO<sub>2</sub> the laser structured area was chipping off the wafer (Fig. 1, lower inset). The ablation started at the Si surface below the SiO<sub>2</sub> layer, and the created plasma and shock wave removed the oxide. In the second approach we change the ablation strategy

<sup>1</sup>Research Centre for Microtechnology, Vorarlberg University of Applied Sciences, Hochschulstraße 1, 6850 Dornbirn, Austria

<sup>2</sup>Institute of Electronics and Photonics, Slovak University of Technology, Ilkovicova 3, 812 19 Bratislava, Slovakia

<sup>3</sup>V-Research GmbH, Stadtstraße 33, 6850 Dornbirn, Austria

<sup>4</sup> Institute of Informatics, Slovak Academy of Sciences, Dubravska cesta 9, 845 07 Bratislava, Slovakia

ivan.hotovy@stuba.sk

and continued with two alternative methods. First, LIPSS were generated directly on a Si wafer and the

oxide layer with a thickness of 350 nm was produced by thermal oxidation on top of the LIPSS subsequently.

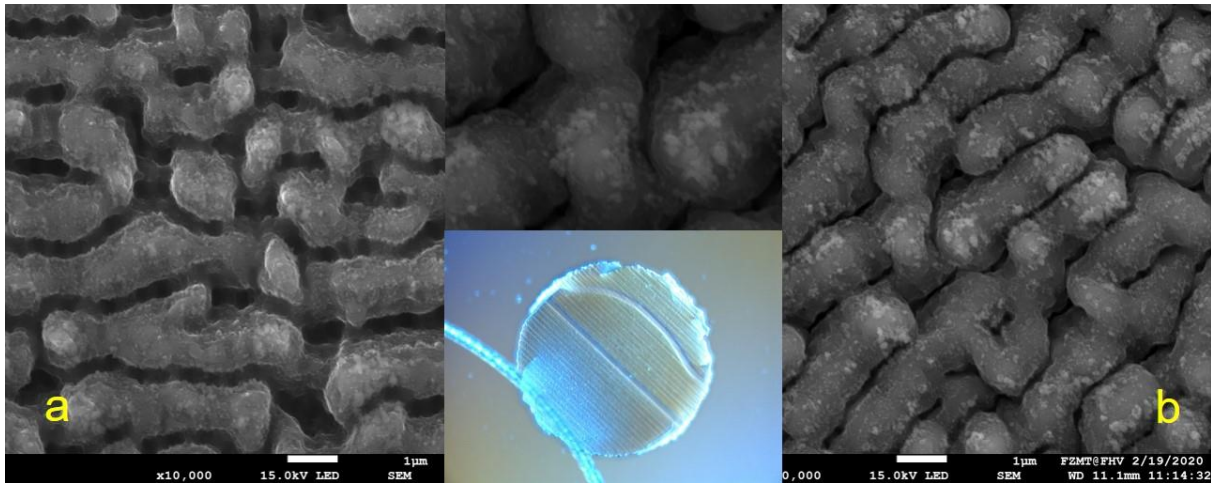


**Fig. 1.** LIPSS on Si with sintered debris (a); thermal oxide with spongy debris inclusions (b)

In the ablation process  $\text{SiO}_2$  debris particles are produced. Most of the oxide particles are removed by an assisting air flow. Yet the remaining traces were sintered onto the Si surface in the next subsequent scans. To form the LIPSS five consecutive scans were required, accumulating the remaining debris in small laser sintered oxide clusters (Fig. 1a). We observed that the isolation quality of the thermal oxide was reduced by these spongy remains (Fig. 1b, and upper inset in Fig. 1). Consequently, this method is not suitable for our gas sensor applications. In our third approach it was possible to solve this problem by replacing the thermal  $\text{SiO}_2$  with an  $\text{Si}_3\text{N}_4$  layer.

### 3 Electrical and gas sensing properties of NiO on LIPSS

As the base material for LIPSS structuring a standard 4-inch silicon wafer was used. Silicon nitride as an electrical barrier layer with a thickness of about 100 nm was deposited onto the LIPSS by PECVD method. Subsequently, NiO layers with a thickness of about 50 nm were sputtered onto micropatterned substrates. The NiO films were deposited by DC reactive magnetron sputtering from a Ni target in a mixture of oxygen and argon. The relative partial pressure of oxygen in the reactive mixture  $\text{O}_2\text{-Ar}$  was 30%. In order to stabilize the properties of NiO thin films, the samples were annealed in a furnace at 500 °C in nitrogen atmosphere for 1 hour. In the final step, several selected samples were coated by Au contact films through a shadow mask for electrical and gas sensing characterization. The surface morphology of the prepared

structures was observed in the field emission scanning electron microscope (FE SEM) Quanta FEG 250 (FEI). The electrical properties of the prepared films were investigated in Van der Pauw geometry. The response from NiO sensors towards hydrogen and acetone was obtained by measuring the electrical resistance by an Agilent 34410A multimeter using a GPIB interface for communication with a computer by LabView platform. Programmable DC Power supply TP-3303U (Twintex) was used as a power supply of the heater element. In all experiments the operation temperature of the sensor was set to 250 °C.

Since the gas sensing elements were prepared directly on LIPSS, SEM observation was also done on this type to identify the effective morphology (Fig. 2). It was observed that the NiO surface reflected the microstructured Si substrate morphology. The NiO film consisting of an agglomeration of small nanosized grains with arbitrary form was created on LIPSS. Nanostructured NiO film consistently covers every available plane. NiO grows not only on top of the LIPSS but also on the sides and valleys of LIPSS and fills the space between the individual microstructures (Fig. 3a). SEM cross sectional images showed the polycrystalline nature of NiO. In this case, NiO thin film is continuous and is created by repeated nanocrystals which homogeneously cover the LIPSS surface (Fig. 3b). In Fig. 4 is a recorded XRD diffractogram from the sample of NiO/ $\text{Si}_3\text{N}_4$  on LIPSS, which confirms the presence of a cubic polycrystalline NiO phase. The diffraction peaks of the NiO thin film were identified and compared on the basis of (fcc) NiO structure (PDF card No. 47-1049).

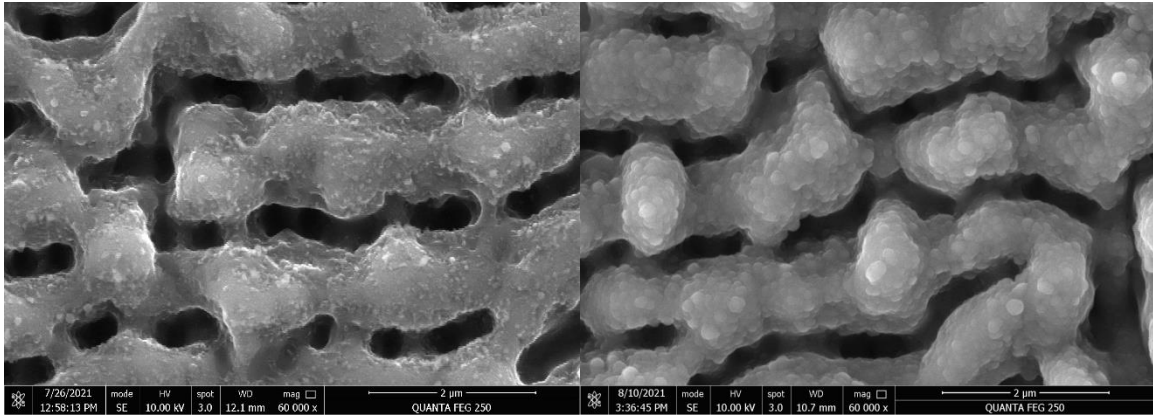


**Fig. 2.** Field emission SEM images of LIPSS structure before (a), and after  $\text{Si}_3\text{N}_4$  deposition (b)

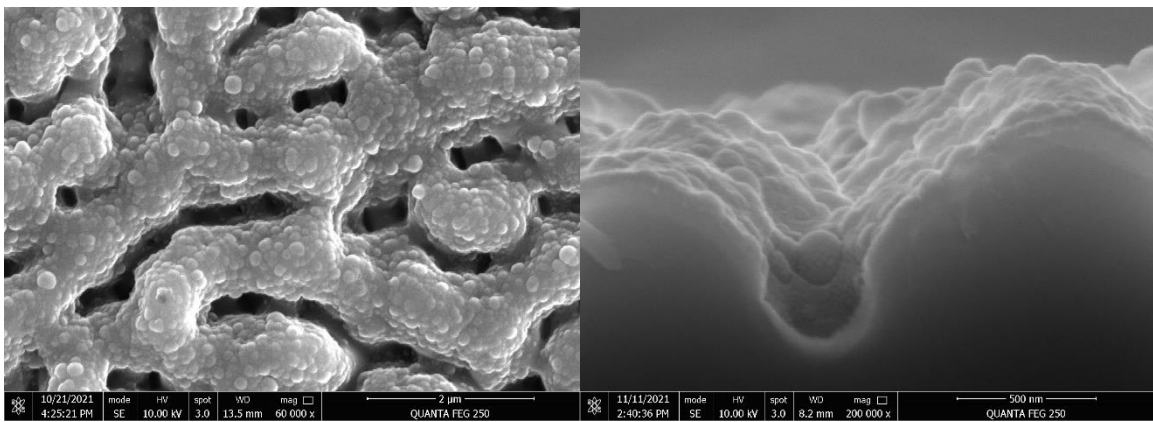


**Fig. 3.** Field emission SEM image after NiO deposition (a), and detailed cross section of LIPSS (b)

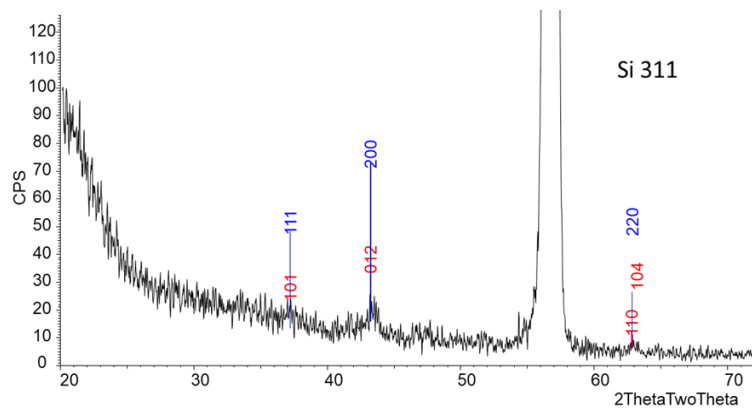


**Fig. 4.** XRD patterns of NiO films with  $\text{Si}_3\text{N}_4$  on LIPSS

The conductance of the prepared NiO films on LIPSS under study was about  $10^{-9}$  S at room temperature. It was found that the conductance of as-deposited NiO films were higher by three orders of magnitude than of the annealed films. Hall measurements confirmed that our NiO films are p-type of semiconductors, wherein the carrier density was in the order of  $10^{13} \text{ cm}^{-3}$  and the mobilities were  $5.54 \text{ cm}^2\text{V}^{-1}\text{s}^{-1}$ . The conductivity of

semiconductor thin films depends on temperature and can be determined by Arrhenius' equation. The temperature variation of the conductance in air has been measured between 25 and 300 °C. It was found that the NiO conductance increased by three orders of magnitude in this temperature range, and NiO samples were p-type semiconductors (Fig. 5).

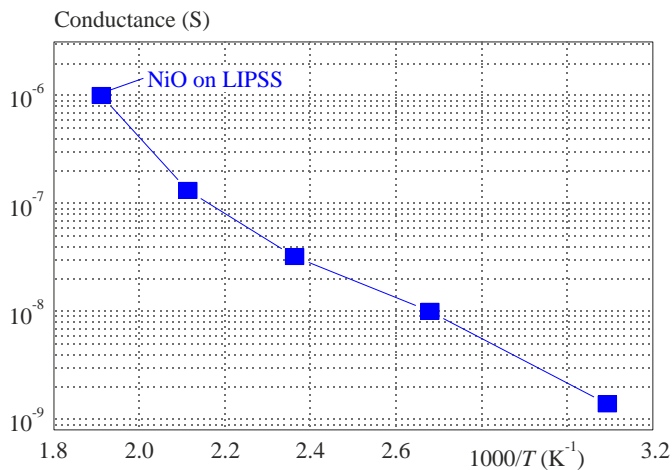


**Fig. 5.** Measured conductance of NiO films on LIPSS with  $\text{Si}_3\text{N}_4$  versus inverse temperature

The gas sensing responses of NiO on LIPSS with an insulating  $\text{Si}_3\text{N}_4$  layer were measured to hydrogen with 500 ppm concentration and acetone with 1000 ppm. The working temperature  $250^\circ\text{C}$  was used and it was optimized for sputtered NiO films in our previous work [11]. Typical response dynamics curves of NiO film and annealed at  $500^\circ\text{C}$  towards hydrogen and acetone is shown in Fig. 6. We noted a change in resistance from  $150\text{ M}\Omega$  to  $350\text{ M}\Omega$  in the case of hydrogen detection and from  $71\text{ M}\Omega$  to  $166\text{ M}\Omega$  in acetone detection. From the given values it is possible to calculate the sensitivity, which in the case of hydrogen represents a sensitivity value of  $400\text{ k}\Omega/\text{ppm}$  and for acetone  $95\text{ k}\Omega/\text{ppm}$ . The recorded 4.2-fold higher sensitivity to hydrogen compared to acetone is not surprising as hydrogen is a purely reducing gas and this finding is consistent with our previous observations [11, 12] valid for NiO deposition on a compact  $\text{Al}_2\text{O}_3$  substrate.

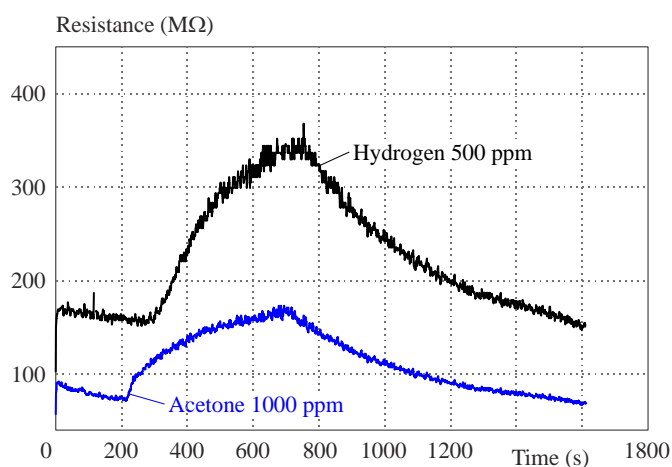


**Fig. 6.** Response dynamics curves of NiO film on LIPSS to hydrogen and acetone at operation temperature of  $250^\circ\text{C}$

## 4 Conclusion

We demonstrated the great potential of laser induced periodic surface structures for surface functionalization and gas sensor applications. Electrical measurements indicate that the samples prepared by LIPSS generation on Si and subsequent thermal oxidation create locally spongy structures with low ohmic resistivity. Therefore, we used an insulating  $\text{Si}_3\text{N}_4$  layer for a working gas sensor demonstrator with enlarged surface area by LIPSS generated on Si.

## Acknowledgement

This work was supported by the Action Austria-Slovakia No. 2022-03-15-002 “Novel Structures for Gas Sensors and Photonic Data Processing Concepts” from the Austrian Agency for International Cooperation in Education and Research (OeAD-GmbH) and by the Scientific Grant Agency of the Ministry of Education of the Slovak Republic and of the Slovak Academy of Sciences, No. 1/0789/21, and by the Slovak Research and Development Agency under contract, No. APVV-21-0278.

## References

- [1] Z. Chen, Z. Chen, Z. Song, W. Ye, and Z. Fan, “Smart gas sensor arrays powered by artificial intelligence,” *Journal of Semiconductors*, vol. 40, no. 11, p. 111601, 2019. doi:10.1088/1674-4926/40/11/111601
- [2] M. Penza and G. Cassano, “Chemometric characterization of Italian wines by thin-film multisensors array and artificial neural networks,” *Food Chemistry*, vol. 86, no. 2, pp. 283–296, 2004. doi:10.1016/j.foodchem.2003.09.027
- [3] S. Sironi and R. Del Rosso, “Smart gas sensor arrays powered by artificial intelligence,” *Sensors*, vol. 14, no. 11, pp. 19979–20007, 2014. doi:10.3390/s141119979
- [4] M. Hakim *et al.*, “Volatile organic compounds of lung cancer and possible biochemical pathways,” *Chemical Reviews*, vol. 112, no. 11, pp. 5949–5966, 2012. doi:10.1021/cr300174a
- [5] J. Chen *et al.*, “Ultra-Low-Power smart electronic nose system based on three-dimensional tin oxide nanotube arrays,” *ACS Nano*, vol. 12, no. 6, pp. 6079–6088, 2018. doi:10.1021/acsnano.8b02371
- [6] H. J. Park *et al.*, “Highly flexible, Mechanically stable, and sensitive  $\text{NO}_2$  gas sensors based on reduced graphene oxide nanofibrous mesh fabric for flexible electronics,” *Sensors and Actuators B: Chemical*, vol. 257, pp. 846–852, 2018. doi:10.1016/j.snb.2017.11.032
- [7] D. Yan *et al.*, “Electrochemical synthesis and the gas-sensing properties of the  $\text{Cu}_2\text{O}$  nanofilms/porous silicon hybrid structure,” *Sensors and Actuators B: Chemical*, vol. 223, pp. 626–633, 2016. doi:10.1016/j.snb.2015.09.080
- [8] M. Leber *et al.*, “Different methods to alter surface morphology of high aspect ratio structures,” *Applied Surface Science*, vol. 365, pp. 180–190, 2016. doi:10.1016/j.apsusc.2016.01.008
- [9] M. Stubenrauch *et al.*, “Black silicon – new functionalities in microsystems,” *Journal of Micromechanics and Microengineering*, vol. 16, no. 6, 2006. doi:10.1088/0960-1317/16/6/s13

- [10] J. Bonse, "Quo vadis LIPSS? – recent and future trends on laser-induced periodic surface structures," *Nanomaterials*, vol. 10, no. 10, p. 1950, 2020. doi:10.3390/nano10101950
- [11] I. Hotovy, L. Spiess, M. Predanocy, V. Rehacek, and J. Racko, "Sputtered nanocrystalline NiO thin films for very low ethanol detection," *Vacuum*, vol. 107, pp. 129–131, 2014. doi:10.1016/j.vacuum.2014.04.012
- [12] I. Hotovy *et al.*, "Preparation and gas-sensing properties of very thin sputtered NiO films," *Journal of Electrical Engineering*, vol. 72, no. 1, pp. 61–65, 2021. doi:10.2478/jee-2021-0009

Received 1 December 2023

---